

Fibrillar templates and soft phases in systems with short-range dipolar and long-range interactions

C.J. Olson Reichhardt, C. Reichhardt, and A.R. Bishop
Theoretical Division, Los Alamos National Laboratory, Los Alamos, New Mexico 87545
 (October 29, 2018)

We analyze the thermal fluctuations of particles that have a short-range dipolar attraction and a long-range repulsion. In an inhomogeneous particle density region, or “soft phase,” filamentary patterns appear which are destroyed only at very high temperatures. The filaments act as a fluctuating template for correlated percolation in which low-energy excitations can move through the stable pattern by local rearrangements. At intermediate temperatures, dynamically averaged checkerboard states appear. We discuss possible implications for cuprate superconducting and related materials.

PACS numbers: 73.50.-h, 71.10.Hf

Mesoscopic and inhomogeneous ordering of charges in diverse materials such as high- T_c superconductors [1], colossal magnetoresistant manganites [2,3], and two-dimensional (2D) electron gas systems [4] is a subject of intense recent study, as such ordered phases may be highly relevant for understanding the properties of these materials, including superconductivity mechanisms, pseudo gaps, transport responses, and magnetic responses. Such phases include labyrinths, stripes, and clusters, and often consist of intermediately ordered patterns, lying between completely ordered and completely disordered systems [5]. Inhomogeneous charge ordering phases can be produced by a competition between repulsive and attractive interactions. In the case of the metal oxides, holes with a repulsive Coulomb interaction move in an antiferromagnetic background, with the distortion of the spins giving rise to a dipolar attraction between holes, and allowing the formation of clump, Wigner crystal, and stripe phases. A variety of other microscopic mechanisms that produce a similar coexistence of long-range repulsion competing with directional short range attraction occur in a wide range of systems, such as defects or dislocations in elastic media, covalent glasses [6], and systems with a finite density of Jahn-Teller polarons [7]. Systems with effective competing repulsive-attractive interactions are abundant in soft matter, where bubble and stripe phases are observed [8]. A particularly relevant issue in these inhomogeneous systems is the role of temperature. Open questions include how the mesoscopically ordered patterns fluctuate or melt, and what the relevant dynamical modes are. Another important issue is what measures best characterize these systems. Temperature effects are particularly important since dynamical and morphological changes along filaments couple to changes in the material properties of the sample.

In this work we focus on the thermal properties of a quasiclassical model for charge ordering of holes in transition metal oxides, in which the particles have a Coulomb repulsion and a dipolar attraction. As a function of hole density (doping) we observe an extended region that we term a “soft phase” comprised of partially ordered filaments. Ordered clumps form for densities below this

region, and ordered stripes (Wigner crystal-like phases) occur above it. We find that the soft filamentary structures persist to high temperatures. Within the soft phase region there is a low temperature onset of motion along the filaments coupled with fluctuations of the filamentary structures. The filaments act as a template for *correlated percolation* of particle motion. When the particle positions are averaged over long times, the filaments form an ordered checkerboard pattern. We have also considered a simpler model of long-range repulsion and *isotropic* short range attraction, and again find evidence for a filamentary soft phase, suggesting that the presence of soft phases with low temperature correlated percolation may be a generic feature of systems with competing long/short range interactions. However, the filamentary soft phase is amplified by the anisotropy (e.g. dipolar in this present case), and the dynamics is typically softer on filaments than in clusters.

Our phenomenological model for the holes consists of particles with competing long-range and short-range interactions [10]. Four charge-ordering phases arise depending on the hole density and the strength of a dipolar interaction induced by the holes: a Wigner crystal; a diagonal stripe phase; an intermediate geometric phase; and at low hole densities and larger dipole interaction strengths, a clump phase. The transitions among these four phases have been studied in simulations [11,12]. We tune the doping level in our model by directly varying the hole density in a rectangular computational box of size $L_x \times L_y$, with L_x and L_y up to 100 unit cells in a CuO_2 plane. We initialize the simulation by placing the holes at random and assigning each hole a magnetic dipole moment of fixed size but random direction. We use an efficient Monte Carlo method to find the minimum of the total potential in this system [12].

We base our model for the interaction between the charges on the spin density wave picture of the transition metal oxides. Full details of the model can be found in [11,12]. The effective interaction between two holes, 1 and 2, a distance \mathbf{r} apart, where r is relaxed to an arbitrary (continuous, off-lattice) value, is given by

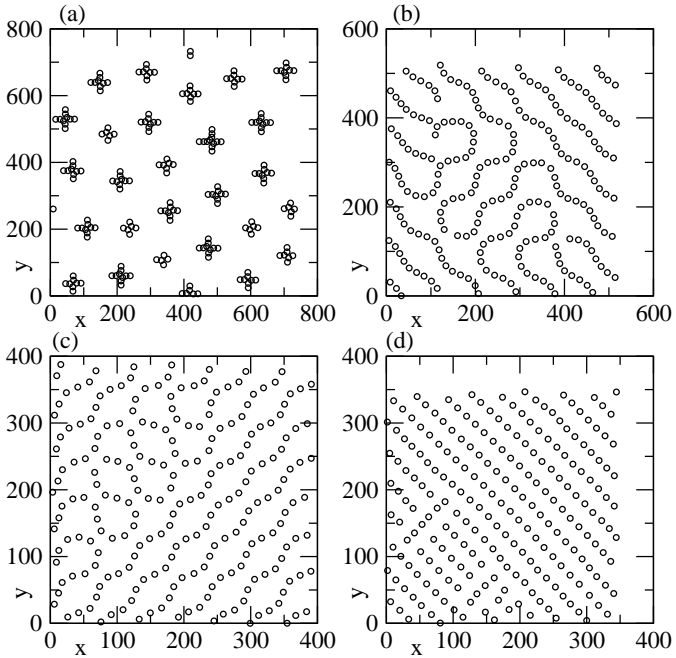


FIG. 1. Static positions of holes for different densities. (a) Clump phase, $n = 0.6$, (b) soft phase, $n = 1.2$, (c) soft phase, $n = 2.1$, (d) anisotropic Wigner crystal phase, $n = 2.7$.

$$V(\vec{r}) = \frac{q^2}{\tilde{r}} - Ae^{-\tilde{r}/a} - B \cos(2\theta - \phi_1 - \phi_2)e^{-\tilde{r}/\xi}. \quad (1)$$

Here, $q = 1$ is the hole charge, θ is the angle between \mathbf{r} and a fixed axis, and $\phi_{1,2}$ are the angles of the magnetic dipoles relative to the same fixed axis, which we assume can take an arbitrary value. A is the strength of the short-range anisotropic interaction, and B is that of the magnetic dipolar interaction [$B \approx A/(2\pi\xi^2)$], which we assume to be independent variables. Throughout this work we take $A = 0$. For the magnetic correlation length, we assume the approximate dependence $\xi = 3.8/\sqrt{n}$ Å; however, in order to observe a larger number of clusters for a fixed number of holes $N = 225$, we artificially reduce the value of ξ to a smaller value ξ' , with $\xi' = \sqrt{0.15}\xi$. Test simulations on much larger systems of 2000 particles with the full screening length indicate that the physics is qualitatively unchanged by this screening length reduction. The distance \tilde{r} is measured in units of the cuprate lattice spacing $a_0 = 3.8$ Å, and the hole density is given by n . The sample is periodic in the $x - y$ plane [17].

We first consider the static hole configurations, illustrated in Fig. 1, obtained at different hole densities by annealing the system from a high temperature. At low densities, cross-like clumps form and organize into an ordered lattice structure [Fig. 1(a)]. Above a density of $n = 0.9$ the clumps begin to touch and are replaced by partially disordered filamentary patterns of the type illustrated in Fig. 2(b) for $n = 1.2$ and Fig. 1(c) for $n = 2.1$. These filamentary patterns persist within a glassy window that extends up to $n = 2.4$, when a more ordered

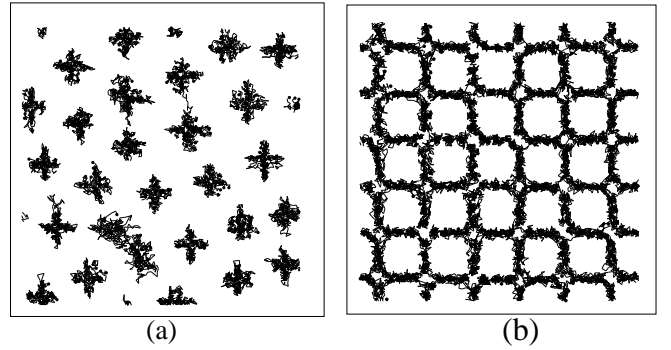


FIG. 2. Image of system above the filamentary melting transition, with lines indicating the motion of the holes between consecutive simulation frames. (a) $n = 0.6$ in the clump phase, where the particles remain predominantly localized. (b) $n = 1.2$ showing the square modulated liquid phase in the filamentary regime.

anisotropic Wigner crystal pattern forms, as shown in Fig. 1(d) for $n = 2.7$.

The transition from the filamentary pattern phase of Fig. 1(b,c) to the anisotropic Wigner crystal phase of Fig. 1(d) occurs when the interactions between the holes become dominated by the Coulomb repulsion. If the system formed a perfect isotropic Wigner crystal, the lattice constant of this crystal would be $r_{WC} = L_x/\sqrt{N}$. We can estimate the density at which the transition occurs by a balance of forces, $q^2/\tilde{r}_{WC}^2 \approx B/\xi$. This becomes $a_0^2/B = r_{WC}$, giving $n = \sqrt{10B/a_0}$, or $n = 2.3$ for the parameters considered here, in reasonable agreement with the transition observed in the simulations.

We next consider the role of temperature-induced fluctuations of these patterns. For the clump region seen in Fig. 1(a), the superlattice clump structure remains stable up to a very high temperature. The superlattice and clumps break up simultaneously around $T_m = 930$ K, where the melting temperature T_m is measured by the onset of diffusion (see inset to Fig. 4). In general particles are confined within the clump up to this temperature, although occasionally a particle can escape from the edge of clump and move to another clump. Such limited motion of particles within the clumps begins at around 700K. The anisotropic Wigner crystal phases found at densities $n > 2.4$ beyond the filamentary soft phase are stable up to about 700K. Above this temperature the entire pattern melts rapidly, although we have not determined the order of this transition.

We now consider the fluctuations within the soft phase. Well below T_m , we find a modulated liquid phase, in which the charges are constrained to remain within a filamentary square pattern, but are free to move along the filaments. This is illustrated in Fig. 2(b) for $n = 1.2$ in the soft phase, showing the holes moving along a square pattern. The pattern is oriented with the simulation box due to the residual dipoles, which form because we have not restricted the spin on each charge to take discrete

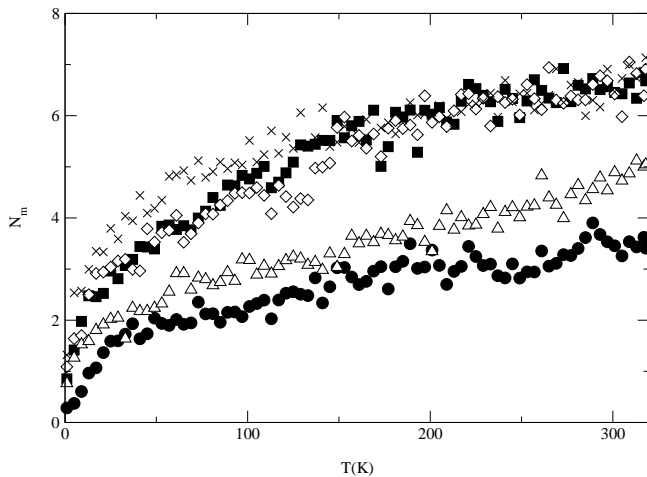


FIG. 3. Pattern reorientation measure N_m as a function of temperature for different hole densities: filled circles, $n = 0.75$, filled squares, $n = 1.2$, open diamonds, $n = 1.65$, x's, $n = 2.25$, and open triangles, $n = 2.7$.

values but have instead allowed the angles to vary continuously. The dipoles align along $\pm 45^\circ$, and thus the system is divided into two equal but interconnected basins of magnetization. We contrast the filamentary square pattern observed throughout the soft phase with a similar image of the clump phase, shown in Fig. 2(a) for $n = 0.6$. Here the holes remain localized within each clump.

The modulated liquid phase remains stable up to the temperature T_m at which the pattern itself is destroyed. We can define a second, lower melting temperature T_s at which the onset of the square (checkerboard) fluid phase, or modulated liquid, occurs. In this modulated liquid phase the particle motion is constrained to follow the square template. Although the hole density is not high enough to create this square structure in the static configuration, when the holes are moving their effective density increases, allowing them to form the square state. At any moment the square state is not fully formed; in a snapshot of the system, the square state contains imperfections and density modulations. On average over time, however, the square state is present, and the particles move in response to its structure.

The temperature T_s at which the square modulated liquid appears varies with doping. More disordered hole configurations (such as $n = 1.2$) have a lower T_s than more ordered configurations (such as $n = 2.7$). To quantify this, we must detect the transition to the modulated liquid. The onset of the modulation occurs when the structure of the pattern begins to change globally due to local rearrangements of the holes. For example, for $n = 1.2$, one of the loops may open and reconnect into a new loop formed out of a previously straight segment. We can detect changes in the structure of the pattern by monitoring the local orientation Θ_v (in the range $[0, \pi/2)$) of a Voronoi polygon centered on each particle

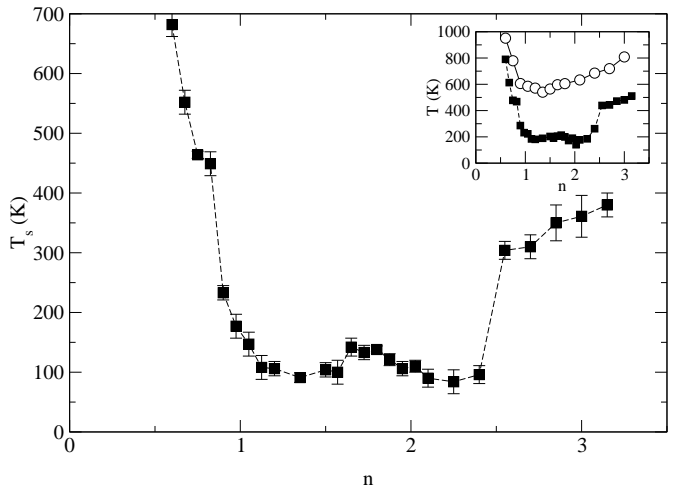


FIG. 4. Onset temperature T_s of modulated square liquid state as a function of hole density n . Inset: Melting temperature of pattern T_m (open circles), and T_s (black squares).

at fixed T . Changes in the pattern orientation produce increased fluctuations of the local orientation $\langle \sqrt{\Theta_v^2} \rangle$. We find the number of particles N_m undergoing pattern changes by counting the particles that have $\langle \sqrt{\Theta_v^2} \rangle \geq 0.2\pi$ during a fixed number of MC steps. The onset of the modulated liquid should occur when enough particles are fluctuating on average to allow the excitations to percolate through the system. If the holes are spaced ξ' from each other along a line, $L_x/\xi' = 38$ holes fit across the sample length, in $N\xi'/L_x = 5.9$ rows of closely packed particles. We therefore select $N_m = 6$ as the filamentary transition, since this would allow one fluctuation at each crossing point of the square pattern to extend across the system. The temperatures T_s obtained with this value of N_m agree well with the onset of the modulated liquid phase as observed through animations of the simulations. We find a clear decrease of T_s in the soft phase when the modulated liquid appears, as illustrated in Fig. 3.

We plot T_s as a function of density in Fig. 4, as determined from measurements of N_m . We find a dramatic decrease in T_s over a soft window from $n = 0.9$ to $n = 2.4$. This corresponds to the geometrically disordered percolation phase. Outside of this soft window, particle motion does not occur until significantly higher temperatures are reached, especially for $n < 0.9$. Using different values of N_m to determine T_s does not alter the range of densities at which the soft window appears; it merely shifts the curve slightly in temperature.

In the soft window, we observe *correlated* percolation. *The onset of structural percolation coincides with a highly directional softness.* This is in contrast to the isotropic melting that occurs at much higher temperatures. Thus, we have a system which contains a *rigid* template of *soft* filaments. At T_s , a type of dislocation mobility transition occurs in which a bundle excitation becomes delocalized. In this case, because the effective interaction between

particles along the chain is highly nonlinear, propagation of a soliton-like excitation can occur, resulting in the time-averaged square pattern.

In the model considered here, the short-range attractive interaction between particles has a strong directional dependence. We have also studied a system with isotropic short range attractive interactions [18], and find that in the stripe phase, melting first occurs along the length of each stripe. We have measured the melting temperature T_m of the three phases in the isotropic model by computing the particle diffusion at each temperature. Particles diffuse freely within the stripes but do not enter the regions between the stripes until higher temperatures. In this system the stripe structure is not filamentary, so only constrained two-dimensional motion of the particles within the broad stripe cluster is possible. T_m is lower in the stripe phase; however, we do not find as dramatic a decrease in T_m due to the quasi-two-dimensional nature of the particle motions within the stripe.

We now discuss some implications of our results for experiments on metal-oxide materials. Our results indicate that the charge-ordered states should persist up to very high temperatures. Signatures of disordered filamentary states occur at much lower temperatures with a transition to a square (checkerboard) state at intermediate temperatures. However, the short/long-range interactions only appear upon (polaron-like) localization of holes, which onsets at the “pseudogap temperature.” Above this temperature, a more metallic electronic state is expected. The square phase that we observe is a time-averaged, not a static, structure, so we predict that it would be detected in experiments such as STM which resolve time-averaged images, and it may be a good template for the STM images observed in doped cuprates [19,20]. Short-time imaging techniques may reveal only disordered structures. The low temperature phase at $T < T_s$ is not fluctuating strongly, and thus appears more disordered than the square phase at $T > T_s$, which could lead to an observable disorder-order “transition” with increasing T . Noise measurements could also detect the onset of the square modulated liquid phase: in the clump phase there should be little noise, while in the modulated liquid phase, large scale fluctuations of the patterns should produce increased noise. It is also likely that external fields will easily induce currents along the filamentary paths in the soft phase. The soft phase at $T_s < T < T_m$ also shows similarities with the inhomogenous states observed in manganites between the true critical temperature T_c and a higher temperature T^* at which short-range order first appears [3].

Some stripe-based theories for superconductivity require fluctuating stripes [21]. In our system, we find that the soft regions (which appear in an intermediate doping region) dynamically fluctuate at low T . Our soft phase could then correspond to the fluctuating stripe regime. An important feature of the soft phase we ob-

serve is that the fluctuations are predominantly on percolating filaments rather than meandering of the filaments themselves. The fluctuating checkerboard state may thus provide a good theoretical starting point for introducing quantum mechanical effects.

In summary, we have considered a model 2D system with competing long-range and directional short-range interactions. We find a soft filamentary or fibrillar regime that occurs at densities between a low-density clump phase and a high-density anisotropic crystalline phase. This soft phase consists of partially ordered filamentary patterns of charges. At low temperatures, the filamentary patterns act as a rigid template for a correlated percolation of particles along the pattern: within the soft phase, the onset of motion occurs at a far lower temperature than that for melting the template backbone. (Quantum-mechanical mesoscopic tunneling of the template can occur but at much slower rates.) We have also found a similar soft phase for other models with competing long/short range interactions, indicating that these phases may be general features of such systems.

We acknowledge helpful discussions with J.C. Phillips and A.B. Saxena. This work was supported by the US DoE under Contract No. W-7405-ENG-36.

-
- [1] V.J. Emery and S.A. Kivelson, *Physica C* **209**, 597 (1993).
 - [2] M. Uehara *et al.*, *Nature* **399**, 560 (1999).
 - [3] J. Burgy *et al.*, *Phys. Rev. Lett.* **87**, 277202 (2001).
 - [4] E. Fradkin and S.A. Kivelson, *Phys. Rev. B* **59**, 8065 (1999).
 - [5] J.C. Phillips, *Phys. Rev. Lett.* **88**, 216401 (2002).
 - [6] J.C. Phillips, *Phase Transitions and Self-Organization in Electronic and Molecular Networks* (Kluwer, New York, 2001).
 - [7] T. Mertelj, D. Mihailovic, and V. Kabanov (unpublished).
 - [8] M. Seul and D. Andelman, *Science* **267**, 476 (1995).
 - [9] V.J. Emery, S.A. Kivelson, and O.V. Zachar, *Phys. Rev. B* **56**, 6120 (1997).
 - [10] C. Reichhardt, *et al.*, *Phys. Rev. Lett.* **90**, 026401 (2003); *Europhys. Lett.* **61**, 221 (2003).
 - [11] B.P. Stojkovic *et al.*, *Phys. Rev. Lett.* **82**, 4679 (1999).
 - [12] B.P. Stojkovic *et al.*, *Phys. Rev. B* **62**, 4353 (2000).
 - [13] J.R. Schrieffer, X.G. Wen, and S.C. Zhang, *Phys. Rev. B* **39**, 11663 (1989).
 - [14] B.I. Shraiman and E.D. Siggia, *Phys. Rev. B* **40**, 9162 (1989).
 - [15] D.M. Frenkel and W. Hanke, *Phys. Rev. B* **42**, 6711 (1990).
 - [16] S. Chakravarty, B.I. Halperin, and D.R. Nelson, *Phys. Rev. Lett.* **60**, 1057 (1988).
 - [17] N. Grønbech-Jensen, *Int. J. Mod. Phys. C* **7**, 873 (1996).
 - [18] C.J. Olson Reichhardt, C. Reichhardt, I. Martin, and A.R. Bishop, *Physica D*, in press; cond-mat/0301236.
 - [19] J.E. Hoffman *et al.*, *Science* **295**, 466 (2002).
 - [20] C. Howald *et al.*, *Phys. Rev. B* **67**, 014533 (2003).
 - [21] See, e.g., E.W. Carlson, V.J. Emery, S.A. Kivelson, and D. Orgad, cond-mat/0206217, and references therein.